SUPPLEMENTARY INFORMATION

Supplementary Figure Legends

Supplementary Figure 1. MDA5 constructs and electrophoretic mobility shift assays (EMSAs). (A) Schematic representation of the MDA5 constructs used in this study. (B) EMSA of CARD-deleted MDA5 and AU24 RNA on a 6% polyacrylamide gel and stained with SYBR Green. Free RNA migrates at the bottom of the gel (arrow). CARD-deleted constructs have a high pI and do not migrate into the gel unless bound to RNA. At higher protein concentrations, AU24 shifts to slower migrating bands and, like full-length MDA5, multiple supershifted species are apparent (bracket). At the highest protein concentration, RNA-protein complexes remain in the well. (C) EMSA of full-length MDA5 with a mutation in the RNA binding surface of the CTD (K983E) and AU20 RNA. (D) EMSA of the MDA5 helicase construct (see panel *A*) with AU20 RNA. This construct also binds AU24 RNA (not shown). Protein-RNA complexes migrate as a more diffuse band that migrates more slowly as protein concentration is increased. (E) EMSA of full-length MDA5 and poly(I:C) on a 1.2% agarose gel. (F) Quantitation of nucleic acid signal for MDA5/poly(I:C) EMSAs (mean ± SEM of 3 experiments). Bound nucleic acid was calculated by integrating the signal >1.5 kb in each well. MDA5 binds cooperatively to poly(I:C) dsRNA ligands (K_d = 652 ± 34 nM, n = 2.26 ± 0.25). This figure is related to Fig. 1.

Supplementary Figure 2. Error surface projection for the cooperativity parameter (K_{d2}/K_{d1}) in a two site model of AU20 binding to CARD-deleted MDA5 using SV-AUC data. The optimal fit of the sedimentation parameter isotherms (Fig. 2) had a global χ^2 of 0.74 with a K_{d2}/K_{d1} of 0.663 (arrow). F-statistics were used to calculate critical χ^2 thresholds above which, a fit would be outside a particular confidence level (horizontal lines). The cooperativity parameter was then fixed at various values and other parameters floated to determine the best fit. A completely non-

cooperative model predicts K_{d2}/K_{d1} = 4 (black vertical line; see Extended Materials and Methods for derivation) and lies just above the 95% confidence level threshold (2 σ; red horizontal line).

Supplementary Figure 3. Small angle X-ray scattering of MDA5 constructs. For each construct, the one-dimensional scattering profile (left), Kratky plot (middle), and Guinier region (right) is shown. All data are on a relative scale. The Kratky plot is a qualitative measure of foldedness, with globular proteins displaying a compact peak at low scattering angles (q) and unfolded proteins having a continuous rise at higher angles. The linear region of the Guinier plot is used to estimate the radius of gyration (R_g) and the forward scattering (I_0) of a globular protein. Well behaved, globular proteins should have a linear relationship between log(I) and q^2 up to $q \approx 1/R_g$ ($1.3/R_g$ is often used for globular proteins). In the Guinier plots, a linear fit to data between the red points is shown. (A) Zero-concentration extrapolated data for the MDA5 helicase domains. (B) Zero-concentration extrapolated data for the CARD-deleted MDA5 domain. (C) SAXS data for concentrated MDA5 CARDs. (D) SAXS data for MDA5ΔL4 collected at NSLS X9A (top) and, for comparison, data collected at CHESS shortly after protein was eluted from a size-exclusion column (bottom). Both datasets gave similar results during analysis. (E) Scattering from a CARD-deleted MDA5-AU20 complex. This figure is related to Fig. 4.

Supplementary Figure 4. Comparison of three-phase dummy atom models for CARD-deleted MDA5/AU20 SAXS data. The program MONSA (Svergun, 1999) was used to calculate 8 models of the protein-RNA complex using three scattering curves (complex, protein alone and simulated RNA alone) with two protein phases and one RNA phase. (A) Seven of the models are shown superimposed with a modified version of the DAMAVER suite. Protein phases are in green and cyan, while the RNA phase is in magenta. The superimposed beads were mapped

onto a new lattice of DAs with the occupancy of each bead given by the density of superimposed beads surrounding it. This probabilistic model is shown in the middle of the bottom row and is colored blue to red for low to high occupancy. The panel at the right and bottom displays the volume- and probability-filtered model shown in Fig. 5E. Note that while many models have the same basic architecture (an RNA phase sandwiched by protein phases and exposed on one face), the relative orientations of the protein phases around the RNA phase differ leading to loss of definition of one protein phase in the filtered model. (B) Filtered averaged model of the protein phases in *(A)*. While the overall arrangement differs in the complex, the protein phases are relatively consistent with each other. The averaged model has a somewhat more closed cleft when compared to the unliganded protein. This figure is related to Fig. 5.

Supplementary Figure 5. Rigid body modeling of CARD-deleted MDA5:AU20 SAXS data. (A) Helicase domains were docked on a 20 bp RNA using known helicase structures and placing the threonines in motif Ib and motif V within 8 Å of the phosphate at position *i* + 3 and *i*, respectively. Numbers in brackets indicate the residue numbers that motif V of each dimer was docked at, with 1-20 and 21-40 being strand A and B, respectively. The RNA is in rainbow colors from blue (nucleotide 1) to red (nucleotide 40). The CTDs were placed and each model was scored against the SAXS data with SASREF (Petoukhov & Svergun, 2005). The coloring of helicase domains is the same as in Fig. 4. The model with the lowest χ value (model "[21,1]") was further refined against the SAXS data while maintaining the distance constraints between the helicase domains and the RNA, allowing small movements of Hel2 and Hel2i and larger movements of the CTD. (B) Experimental SAXS curve fitted to the calculated SAXS curves for the best rigid body model (model [21,1] from panel *A*, in green) after rigid body refinement (χ = 1.35). (C) MDA5 model generated based on the crystal structures of RIG-I bound to RNA. The

fit of the calculated SAXS curve to the experimental data is shown in *(B)* in blue. (D) The shape parameters for the refined rigid body MDA5 model and the RIG-I based MDA5 model. The RIG-I based model has significantly different shape parameters than the experimentally determined model of the MDA5:RNA complex.

Supplementary Figure 6. Negative stain electron microscopy images of CARD-deleted MDA5/*Φ*6 RNA. (A) Filament bundle of CARD-deleted MDA5/ *Φ*6 RNA. Several examples of bundles were observed for *Φ*6 genomic dsRNA mixed with CARD-deleted MDA5, but not with full-length MDA5. (B) Magnification of region boxed in *(A*). (C) Control specimen containing CARD-deleted MDA5 only. (D) Control specimen containing RNA and cytochrome C. This figure is related to Fig. 6.

Supplementary tables

Supplementary Table I. X-ray diffraction data collection and refinement statistics for MDA5 Hel2i. This table relates to Fig. 3 in the main text.

Dataset	**Native**	**Se-Met MAD**	
Data Collection		Peak	Inflection
Space Group	$P2_12_12_1$	$P2_12_12_1$	
Cell Dimensions *a, b, c* (Å)	23.878, 57.618, 90.332	24.14, 59.396, 89.4	
Wavelength (Å)	1.0750	0.9791	0.9793
Resolution (Å)[a]	50-2.02 (2.09-2.02)	30.00-2.05 (2.12-2.05)	30.00-2.30 (2.38-2.30)
R_{sym} or R_{merge}[a]	0.12 (-)	0.13 (0.49)	0.11 (0.63)
$I / \sigma I$[a]	17.8 (1.9)	23.2 (3.8)	18.2 (2.9)
Completeness (%)[a]	100 (99.9)	92.0 (97.4)	95.9 (97.6)
Redundancy[a]	6.7 (6.8)	12.6 (11.2)	7.1 (6.7)
No. unique reflections	8873	7880	10807
Refinement			
Resolution (Å)	35.6-2.00		
No. reflections (working set)	8387		
No. reflections (test set)	442		
R_{work} / R_{free}	19.3 / 22.2		
N. atoms	1102		
Protein	1047		
Water	39		
Sulfate	15		
Average *B*-factors[b]	41.19 (41.07)		
Protein (Å^2)	41.06 (40.96)		
Water (Å^2)	44.69		
Sulfate (Å^2)	75.3		

RMS[c] deviations	
Bond lengths (Å)	0.002
Bond angles (°)	0.578
Ramachandran plot (%)	
Favored	98.4
Allowed	1.6
Generous	0.0
Disallowed	0.0

[a]Highest resolution shell is shown in parentheses.

[b]Residual B-factors after TLS refinement. See PDB entry for TLS refinement parameters.

[c]RMS, root mean square.

[d]R_{free}, R_{work} with 5% of F_{obs} sequestered before refinement.

Supplementary Table II. Small Angle X-ray Scattering statistics for MDA5 constructs. This table relates to Fig. 4 in the main text.

Construct	Concentration (mg/ml)	I_o/c	R_g (Å)	MW_{BSA} / MW_{exp} (kDa)*	Gnom P(r) used for DA modeling			
					q range (Å^{-1})	D_{max} (Å)	Total Estimate	<NSD> of models
MDA5 helicase	12.4	25.9	37.3					
	6.2	24.8	36.1					
	3.2	23.7	35.1					
	0	23.3	34.3	51/ 65 **	0.0175 – 0.2325	120	0.639	0.74
CARD-deleted MDA5	11.5	31.7	51.0					
	5.8	27.1	45.9					
	2.9	25.4	42.6					
	0	22.8	39.5	75 / 81	0.0165 – 0.1825	135	0.650	0.72
MDA5 CARDs	12.2	10.0	19.5	22 / 23	0.030 – 0.404	65	0.716	0.53
	8.1	12.0	20.2					
	4.3	11.9	20.3					
	1.6	12.8	20.1					
MDA5(ΔL4)	4.6	35	52.1	116 / 114				
	2.6	37.1	50.5	122 / 114				
(fraction from SEC collected at CHESS F2)	2.4	3.5	53.4	104 / 114				
CARD-deleted MDA5/AU20	3.4	87.6	47.1	192 / 173	0.012 – 0.1675	165	0.606	0.66 / 1.42 / 0.75†

*The molecular weight of the sample was calculated with I_o/c for a BSA standard collected during the same data collection period.

**Using the SAXS MoW server (http://www.if.sc.usp.br/~saxs/), which does not rely on concentration measurements or standard comparison, the MW was 72.6 kDa.

†NSD values are for the following: 1-phase model / 3-phase model / 3-phase model, protein phases only.

Extended Materials and Methods

Nucleic acids

Oligonucleotides were synthesized by Sigma-Aldrich or at the W.M. Keck Biotechnology Resource Laboratory at Yale University. AU20 and AU24 have the palindromic sequences 5'-GCAAAUAAGCGCUUAUUUGC and 5'-GCAUAAAUAAGCGCUUAUUUAUGC, respectively. dAU20 and dAU24 are the corresponding DNA oligonucleotides. Oligonucleotides were annealed by heating to 90˚C and slowly cooling to 30 ^{o}C in SPG buffer pH 7.0 (49 mM NaH_2PO_4, 49 mM glycine, 14 mM succinic acid) plus 100 mM KCl and 2 mM $MgCl_2$. Extinction coefficients for dsRNA were calculated as 321.53 and 391.21mM^{-1} cm^{-1} for AU20 and AU24 respectively, assuming hypochromaticity similar to dsDNA. Poly(I:C) RNA was purchased from Midland Certified Reagents. *Φ*6 RNA was prepared with a QIAamp viral RNA kit (Qiagen) from phage grown on *Pseudomonas syringae*, a gift from Paul Turner (Yale University).

Expression and purification of MDA5 constructs

Genes encoding five constructs of mouse MDA5 were cloned in frame with the N-terminal histidine purification tag of a pET28a vector in which the thrombin cleavage site was replaced with a tobacco etch virus (TEV) protease cleavage site. The residue ranges of the mouse MDA5 constructs were as follows: full-length 1-1026; CARDs 1-207; CARD-deleted 304-1026; helicase 304-898; and Hel2i 545-697. In all construct except Hel2i and CARD-deleted MDA5, residues 639-669 were replaced with GSGSG (ΔL4 helicase loop deletion) by site-directed mutagenesis. In Hel2i and CARD-deleted MDA5 residues 646-663 were deleted (ΔL2 loop deletion). *Escherichia coli* Rosetta(DE3) cells (Novagen) were transformed with an MDA5 construct and grown to OD_{600} 0.4-0.5 at 37˚C. After cooling for 15 min at 16˚C, expression was induced overnight with 0.4 mM isopropyl-β-D-1-thiogalactopyranoside (IPTG). Harvested cells were resuspended in SPG buffer pH 6.0 (49 mM NaH_2PO_4, 49 mM glycine, 14 mM succinic acid), 0.4 M KCl, 5 mM β-mercaptoethanol, 5% glycerol, 20 mM imidizole. Roche Complete Protease

Inhibitor (without EDTA), 0.2 mM phenylmethanesulfonylfluoride (PMSF) and 1 µg/ml pepstatin A were added immediately prior to cell lysis. For the expression of the selenomethionine-substituted MDA5 helicase insert domain, the *E. coli* methionine biosynthesis pathway was inhibited as described (Van Duyne et al, 1993).

MDA5 proteins were purified by nickel-affinity chromatography with Ni-NTA agarose (Qiagen). For proteins containing the MDA5 regulatory domain, the sample was further purified using with a HiTrap Q FF anion exchange column (GE Healthcare) to remove contaminating *E. coli* RNA. All proteins were further purified by cation exchange and size-exclusion chromatography with monoS and Superdex 200 10/300 GL columns (GE Healthcare).

Electrophoretic mobility shift assays (EMSAs)

Annealed oligonucleotides were mixed with MDA5 protein and SPG buffer pH 7.4, 0.1 M KCl, 2 mM $MgCl_2$ in a total volume of 10 µl. After 1 h incubation at room temperature, 10x native loading buffer (15% Ficoll with 0.1% Bromophenol Blue in 0.5x Tris-Borate-EDTA (TBE) buffer) was added and the samples were immediately loaded on a 6% PAGE gel and run in 0.5x TBE buffer for 1 h at 100 V. We note that CARD-deleted constructs of MDA5 have a high *pI* and did not migrate into the gel under these conditions without binding to nucleic acid. Nucleic acids were visualized by SYBR Green (Molecular Probes) on a UV lightbox or digitized with a laser scanner for quantitation using 472-nm excitation. For dissociation equilibrium constant (K_d) determination, dsRNA concentration was fixed at 100 nM and protein was titrated from 50 nM to 5 mM. The fraction of bound nucleic acid was determined by integrating the signal intensity in each lane. At low protein concentrations, ligand depletion was corrected for by subtracting the concentration of bound RNA from the total protein concentration (assuming mostly 1:1 binding at low concentrations). Data for three titrations of MDA5ΔL4 with oligonucleotides AU20 and AU24 were averaged and the fraction of RNA bound, *Y*, was fitted to the following equation:

$$Y = \frac{[MDA5]^n}{K_d^n + [MDA5]^n}$$

where *n* is the Hill coefficient. For helicase domain with AU20, for which the protein-RNA complex did not enter the gel, the fraction bound was determined from the ratio of free RNA in each mixture to the total RNA signal in control lanes without protein.

Analytical ultracentrifugation

To determine oligomeric states of MDA5 alone and in complex with various oligonucleotides, we measured the sedimentation velocities of the protein and its complexes with an Optima XL-I analytical ultracentrifuge equipped with both absorbance and interference optical detection systems (Beckman Coulter). CARD-deleted MDA5 was mixed with 1 μM AU20, loaded in the cell assembly and temperature-equilibrated at 20˚C for at least 1 h prior to beginning the run. The protein solution was centrifuged at 20˚C and 45-50 krpm in an An-60 Ti rotor (Beckman-Coulter). Absorption at 260 nm and fringe displacement with interference optics were measured for 6-10 h. Data were fitted to a *c(S)* sedimentation coefficient distribution, which was calculated with Sedfit 12.1 and regularized using the maximum entropy method with a value of 0.7. Values for protein vbar (0.741 ml g^{-1}), buffer density (1.00491 g ml^{-1}) and viscosity (0.01009 P) were calculated with SEDNTERP. For global analysis of data to a binding model, we performed a multisignal sedimentation velocity (MSSV) analysis of the 15:1 μM MDA5:AU20 mixture (Fig. 2B). In this analysis, SV-AUC data of the individual components and the mixture were collected using different optical detection methods (280 nm, 260 nm and fringe displacement). The extinction coefficient of AU20 at 260 nm was fixed at 321.53 mM^{-1} cm^{-1} (RNA showed no signal with interference optics). For the protein component, an extinction coefficient-like parameter for fringe displacement was fixed at 223.283 fringes mM^{-1} and the extinction coefficient at 280 and 260 nm refined using global *c(S)* fitting in the program SEDPHAT. A sedimentation profile, $c_k(S)$,

consistent with each component's spectral properties was then calculated for the mixture using global fitting (Balbo et al, 2005). The area under each peak in the $c_k(S)$ is proportional to the concentration of each component in a particular complex and the ratio of the areas gives the stoichiometry of the complex.

Weight averaged sedimentation coefficient (S_w), reaction boundary sedimentation coefficient ($S_{reaction}$) and population isotherms ($Pop_{undisturbed}/Pop_{reaction}$) were generated from the c(S) distributions calculated from 260 nm SV-AUC data for each mixture using the integration tool of SEDFIT. For the 1.5 μM CARD-deleted MDA, 1 μM AU20 mixture, a Bayesian prior probability was applied to select c(S) profiles consistent with our expectation of a free protein peak at 4.2 S to resolve the undisturbed and reaction boundaries (Brown et al, 2007). Global fitting of isotherms was performed in SEDPHAT using the model $R + P \rightarrow RP + P \rightarrow RP_2$ (R, AU20; P, MDA5) and the extinction coefficients determined in the MSSV experiment. A critical χ threshold was calculated using F-statistics to test the significance of parameter changes. Total competent AU20 RNA concentration was allowed to float, as a contaminant was present sedimenting at 0.8-1 S with similar 260 nm signal for all RNA containing samples. The final RNA concentration was refined to 0.8 μM.

In the non-cooperative, identical binding site model, an individual binding event is described by the microscopic dissociation constant, *k*:

$$k = \frac{[R_{00}][P]}{[R_{0P}]} = \frac{[R_{00}][P]}{[R_{P0}]} = \frac{[R_{P0}][P]}{[R_{PP}]} = \frac{[R_{0P}][P]}{[R_{PP}]}$$

where the receptor RNA (R) has two sites denoted by subscripts that can be filled with one protein molecule (P). The macroscopic dissociation constants, $K_{d\#}$, are given by:

$$K_{d1} = \frac{[R_{00}][P]}{[R_{P0}]+[R_{0P}]} = \frac{1}{2}k$$

$$K_{d2} = \frac{([R_{P0}]+[R_{0P}])[P]}{[R_{PP}]} = 2k$$

Then:

$$\frac{K_{d2}}{K_{d1}} = 4$$

Smaller numbers of this ratio indicate positive cooperativity (subsequent binding events are tighter than expected), whereas larger numbers indicate negative cooperativity (subsequent binding events are weaker than expected).

Crystallization and structure determination of the MDA5 helicase insert domain

Crystals of selenomethionine-substituted or native MDA5 helicase insert domain (MDA5 Hel2i) grew by hanging drop vapor diffusion at 16-20˚C. MDA5 Hel2i at 10-20 g/l in 20 mM HEPES 7.5, 0.2 M KCl, 5 mM β-mercaptoethanol was mixed with an equal volume of SPG buffer pH 8.5-9.5 and 1.9-2.2 M ammonium sulfate. Excess solvent was removed from crystals by passage through paraffin oil before freezing in liquid nitrogen. Crystals belonged to space group $P2_12_12_1$ with one molecule per asymmetric unit. Data were collected at 100 K at the experimentally determined peak anomalous diffraction wavelength of selenomethionine (0.9791 Å) and the anomalous inflection point (0.9793 Å). Phases were determined by multiple-wavelength anomalous diffraction (MAD). Data processing was performed with HKL2000 (Goldschmidt-Clermont et al, 1991). Heavy atom sites were located and experimental phases were calculated with SHELX and HKL2MAP. Buccaneer in the CCP4 suite was used for automated model building. The model was improved with rounds of model building, refinement and water placement with Coot and Phenix. Final refinement included optimization of TLS parameters with REFMAC5 to model anisotropic displacements within the protein, yielding R_{work} and R_{free} of 19% and 22% respectively. 98.4% of all residues are in the most favored regions of the Ramachandran plot, and no residues are in disallowed regions. See Table S1 for data collection and refinement statistics.

Structure determination of MDA5 by small-angle X-ray scattering (SAXS)

MDA5 protein solutions were purified as above and concentrated using Amicon centrifugation concentrators. The flow through from concentration was used as buffer blank for solution scattering. Before data collection, samples were spun for 10 min at 14 krpm. Data were collected at the X9A beam line of the National Synchrotron Light Source with overlapping Pilatus 300k (SAXS) and MarCCD (WAXS) detectors (accessible q range, 0.006-1.7 Å; $q = (4\pi \sin 2\theta) / \lambda$). For each dataset triplicate measurements were collected by flowing 20 µl of sample through a capillary at 14˚C over 30 s. A dilution series for each sample was performed as indicated in Table S2. Bovine serum albumin (BSA) used as a standard for molecular weight calculations. All data reduction and processing were performed with PyXS (http://x9.nsls.bml.gov/software/pyXS.htm). Guinier and P(r) analysis was performed with AUTORG and AUTOGNOM from the ATSAS suite. For constructs containing the helicase domains, Guinier analysis showed increasing I_o/c and R_g with concentration, so linear extrapolation was used to calculate a zero-concentration curve and remove the solution structure factor component.

DA modeling, rigid body modeling and ensemble optimization were performed with ATSAS program suite. Normal mode refinement of the helicase domain structure was performed using the Small Angle Scattering Toolbox (SASTBX; http://sastbx.als.lbl.gov).

Model fitting to data were scored based on χ, where:

$$\chi^2 = \frac{1}{N}\sum\left(\frac{I_{calc} - I_{obs}}{\sigma}\right)^2$$

For DA modeling, a P(r) was calculated using AUTOGNOM and models were calculated with DAMMIF using data to a q-value of $8/R_g$ (see Table S2 for q-range, D_{max} and Total Estimate). Averaging of models was performed using the DAMAVER suite, which superimposes models and calculates the Normalized Spatial Discrepancy (NSD) between models. NSD values around

1 indicate similar models with stable DAMMIF solutions ~0.7. Models with NSD to the other models greater than twice the variation from the overall average <NSD> were discarded during averaging by DAMAVER. For multiphase modeling, three phases (two protein phases and one RNA phase) were defined with volumes based on SAXS data for CARD-deleted MDA5 alone or calculated from a 20-bp poly(A:U) model RNA using CRYSOL (Svergun et al, 1995). A starting ellipsoid DA volume of 120 x 80 x 80 Å was then refined against the protein-RNA, protein alone and (simulated) RNA alone SAXS data. Eight runs were performed and a modified version of the DAMAVER suite (http://www.embl-hamburg.de/~maxim/addon/monsaver.zip) was used to superimpose models, calculate NSDs, and average the models.

Ensemble optimization of the full-length MDA5 dataset was performed using RANCH and GAJOE from the ATSAS suite. 10^5 structures were generated. A 95-amino acid linker was included between the MDA5 CARDS in the Type IV configuration and the SAXS-refined helicase domain model. A 3-amino acid linker was included between the helicase domain and a homology model of mouse MDA5 CTD (based on PDB 3GA3). A genetic selection algorithm was then used to select an ensemble of curves to the SAXS data. Multiple runs were performed using different ensemble sizes, with the best-fit ensembles containing 5-10 structures.

Models of protein-RNA complexes were generated by superposition of the MDA5 Hel1 and Hel2 domains on known nucleic acid-bound helicase structures (PDB IDs 2P6R, 3O8C, 3RC8). The 4 base segment in 2P6R spanning motifs Ib and V was superimposed on one end of a model 20bp poly(A:U) RNA, and the closed MDA5 helicase structure was superimposed such that the conserved Threonine in motifs Ib and V overlapped optimally. All possible positions that maintained contact of the threonine in those motifs with the phosphates at *i* and *i* + 3 along the poly(A:U) RNA were generated by applying a screw translation to the protein corresponding to the helical pitch of A-form RNA (16 possible positions along each strand). After discarding redundant and significantly clashing pairs, 16 model combinations were left (14 combinations on opposite tracking strands, 2 on the same tracking strand). These combinations

were refined in SASREF, fixing Hel1 and the RNA, and allowing small movements of the Hel2 and the insert domain (1 Å translation and 2˚ rotation max/step) and large movements of the CTD (5 Å translation and 20˚ rotation max/step). Distance constraints at domain junctions were maintained and the threonine of motif V in Hel2 had to be within 8 Å of the phosphate backbone at position *i* of the tracking strand. The model with the least structural distortion and best fit to the SAXS data was then chosen for multiple rigid body fitting to test the stability of the solution (n = 8).

To generate a model based on the RIG-I structures determined by Kowalinski et al (2011) (helicase domain bound to 19 bp RNA) and Jiang et al (2011) (helicase domains + CTD bound to 14 bp RNA), the RNA ligand of each RIG-I structure was superimposed onto both ends of an idealized 20 bp duplex. In this configuration the contacts of the helicase domain and CTD were identical to those in the crystal structures and the overall helicase dimer resembled the "[17,37]" MDA5 dimer model that was generated for refinement against the SAXS data (Supplementary Fig. 5A). Homology models of MDA5 domains were then superimposed onto the two RIG-I subunits. To compare this model with those generated and refined with SASREF, the model was run through SASREF while keeping the domains fixed.

Homology Modeling

All homology models were calculated using MODELLER v9.7 (Eswar et al, 2006). Structural alignment of the helicase domains (MDA5 Hel2i and human MDA5 Hel1, PDB 3BE6) to *P. furiosus* Hef helicase (PDB 1WP9) was used to refine sequence alignment. For MDA5 CARDs, a multiple sequence alignment was generated from a structural alignment of CED-4 CARD (PDB 3LQQ), Apaf-1 and procaspase-9 CARDs (PDB 3YGS) and MAVS CARD (PDB 2VGQ). Each MDA5 CARD was manually aligned to the sequence alignment. Regions of the alignments were iteratively adjusted if homology models showed unrealistic or high-energy values. CARD-CARD interfaces were used from the above structures to dock MDA5 CARD1 and CARD2 in

each prototypical interface arrangement. The connecting loop was then built with MODELLER. For the Type II interface, a homology model using duck RIG-I CARDs was built from PDB 4A2Q.

Supplemental References

Balbo A, Minor KH, Velikovsky CA, Mariuzza RA, Peterson CB, Schuck P (2005) Studying multiprotein complexes by multisignal sedimentation velocity analytical ultracentrifugation. *Proceedings of the National Academy of Sciences of the United States of America* **102:** 81-86

Brown PH, Balbo A, Schuck P (2007) Using prior knowledge in the determination of macromolecular size-distributions by analytical ultracentrifugation. *Biomacromolecules* **8:** 2011-2024

Eswar N, Webb B, Marti-Renom MA, Madhusudhan MS, Eramian D, Shen MY, Pieper U, Sali A (2006) Comparative protein structure modeling using Modeller. *Curr Protoc Bioinformatics* **Chapter 5:** Unit 5 6

Goldschmidt-Clermont PJ, Kim JW, Machesky LM, Rhee SG, Pollard TD (1991) Regulation of phospholipase C-gamma 1 by profilin and tyrosine phosphorylation. *Science* **251:** 1231-1233

Svergun D, Barberato C, Koch MHJ (1995) CRYSOL - A program to evaluate x-ray solution scattering of biological macromolecules from atomic coordinates. *Journal of Applied Crystallography* **28:** 768-773

Svergun DI (1999) Restoring low resolution structure of biological macromolecules from solution scattering using simulated annealing. *Biophysical journal* **76:** 2879-2886

Van Duyne GD, Standaert RF, Karplus PA, Schreiber SL, Clardy J (1993) Atomic structures of the human immunophilin FKBP-12 complexes with FK506 and rapamycin. *J Mol Biol* **229:** 105-124

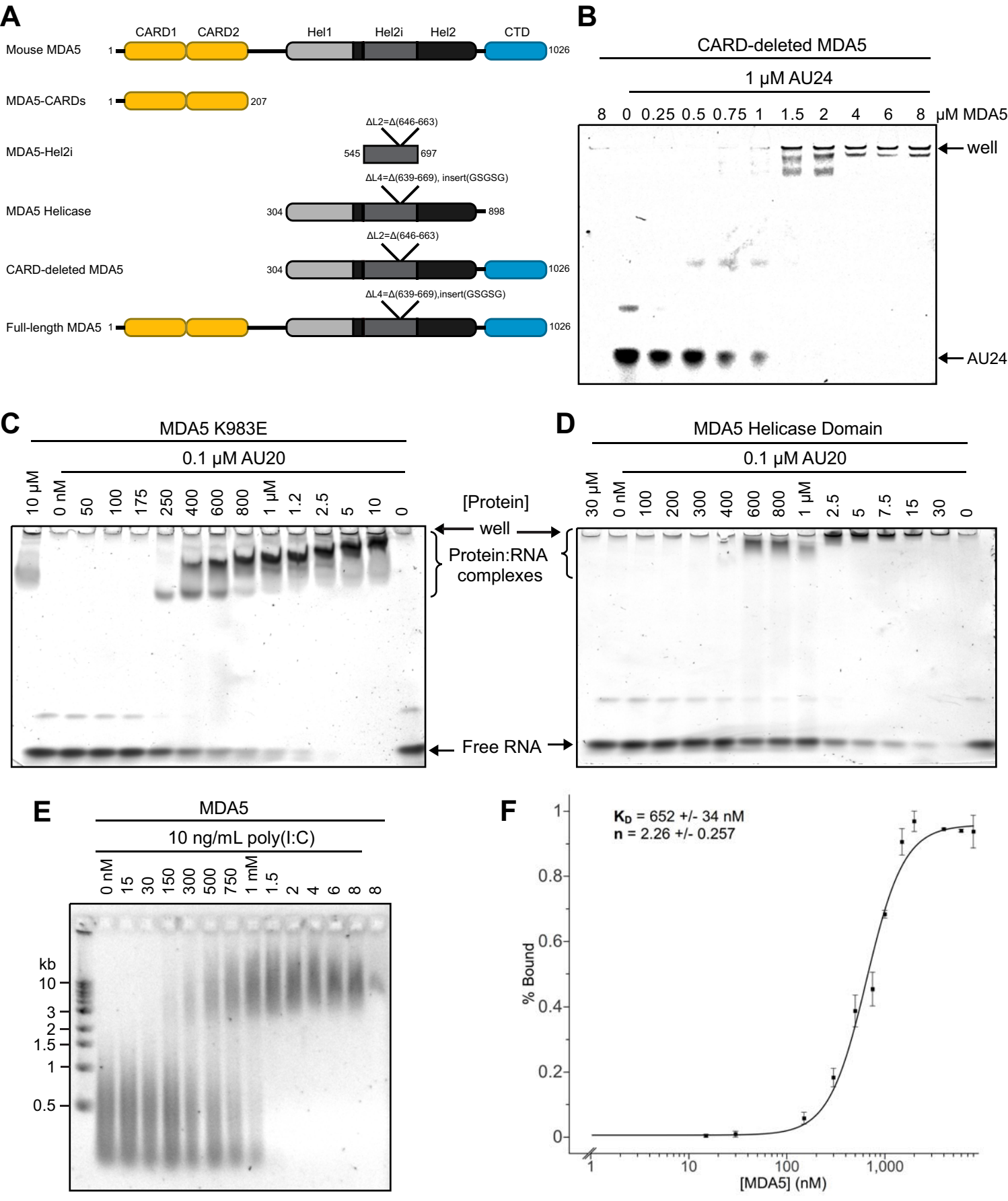
A
CARD1
CARD2
Hel1
Hel2i
Hel2
CTD
Mouse MDA5
1
1026
MDA5-CARDs
207
ΔL2=Δ(646-663)
MDA5-Hel2i
545
697
ΔL4=Δ(639-669), insert(GSGSG)
MDA5 Helicase
304
898
CARD-deleted MDA5
Full-length MDA5
ΔL4=Δ(639-669),insert(GSGSG)
B
CARD-deleted MDA5
1 μM AU24
8 0 0.25 0.5 0.75 1 1.5 2 4 6 8 μM MDA5
well
AU24
C
MDA5 K983E
0.1 μM AU20
10 μM 0 nM 50 100 175 250 400 600 800 1 μM 1.2 2.5 5 10 0
[Protein]
well
Protein:RNA complexes
Free RNA
D
MDA5 Helicase Domain
0.1 μM AU20
30 μM 0 nM 100 200 300 400 600 800 1 μM 2.5 5 7.5 15 30 0
E
MDA5
10 ng/mL poly(I:C)
0 nM 15 30 150 300 500 750 1 mM 1.5 2 4 6 8 8
kb
10
3
2
1.5
1
0.5
F
K_D = 652 +/- 34 nM
n = 2.26 +/- 0.257
% Bound
0
0.2
0.4
0.6
0.8
1
1
10
100
1,000
[MDA5] (nM)

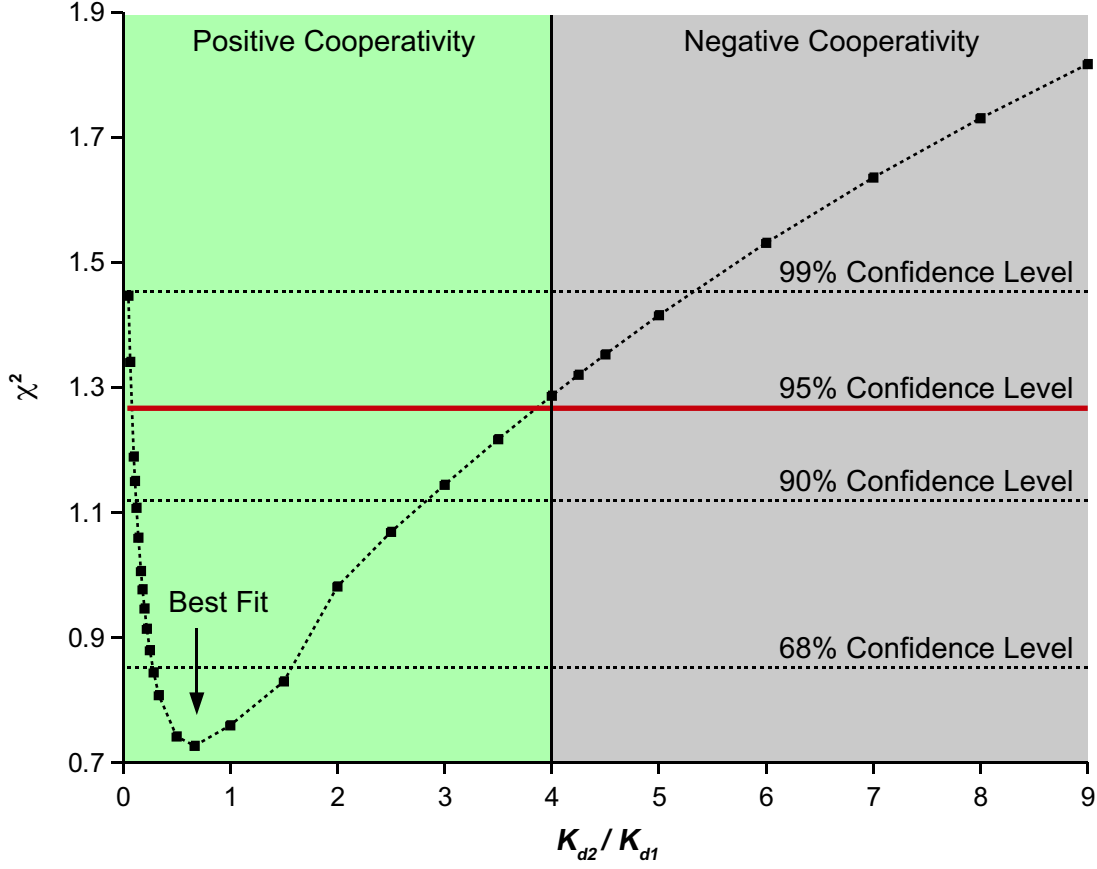
Positive Cooperativity
Negative Cooperativity
99% Confidence Level
95% Confidence Level
90% Confidence Level
68% Confidence Level
Best Fit
χ²
K_d2 / K_d1
1.9
1.7
1.5
1.3
1.1
0.9
0.7
0
1
2
3
4
5
6
7
8
9

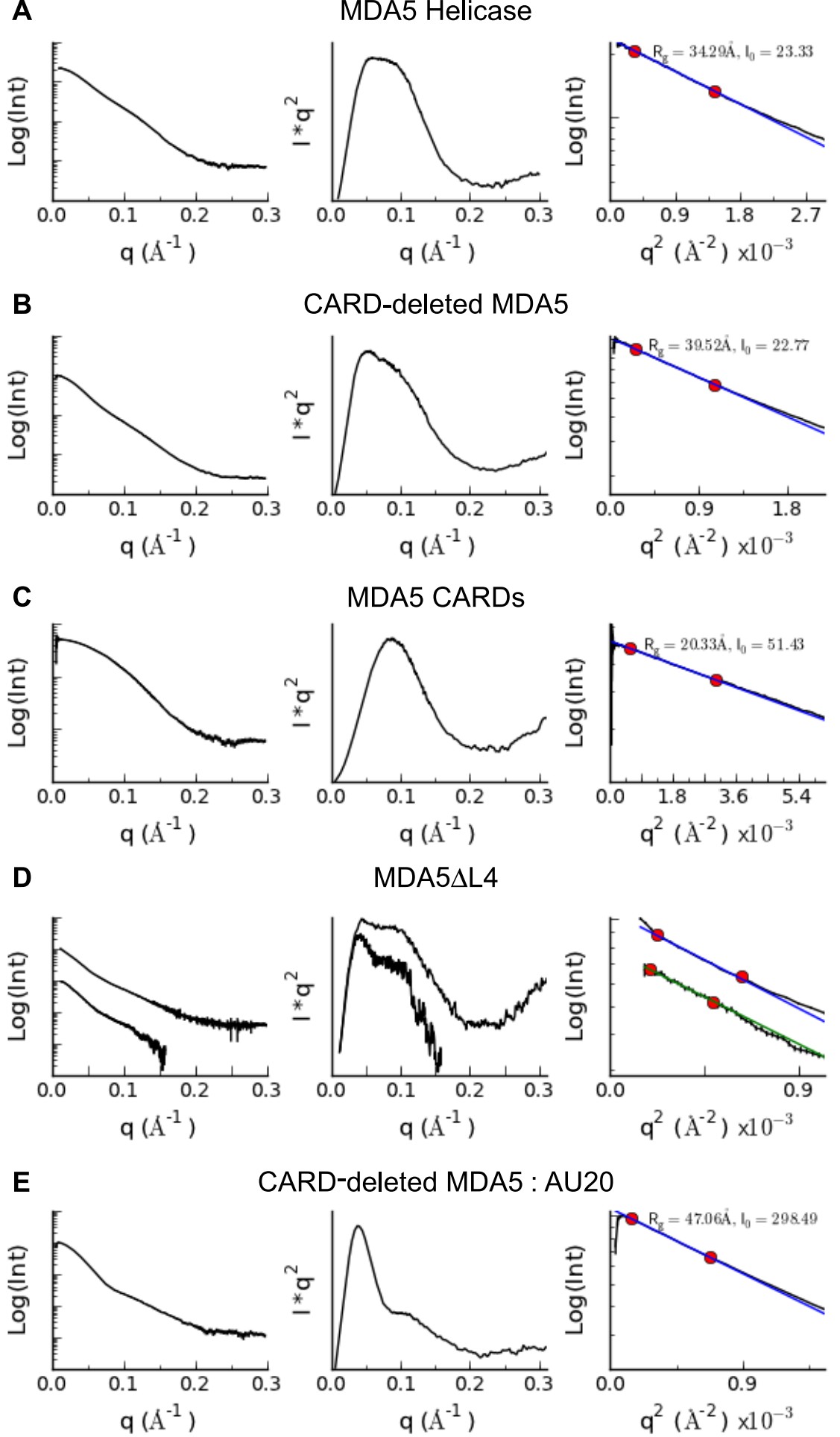
A
MDA5 Helicase
Log(Int)
I*q²
Log(Int)
q (Å⁻¹)
q (Å⁻¹)
q² (Å⁻²) x10⁻³
Rg = 34.29Å, I0 = 23.33
B
CARD-deleted MDA5
Rg = 39.52Å, I0 = 22.77
C
MDA5 CARDs
Rg = 20.33Å, I0 = 51.43
D
MDA5ΔL4
E
CARD-deleted MDA5 : AU20
Rg = 47.06Å, I0 = 298.49

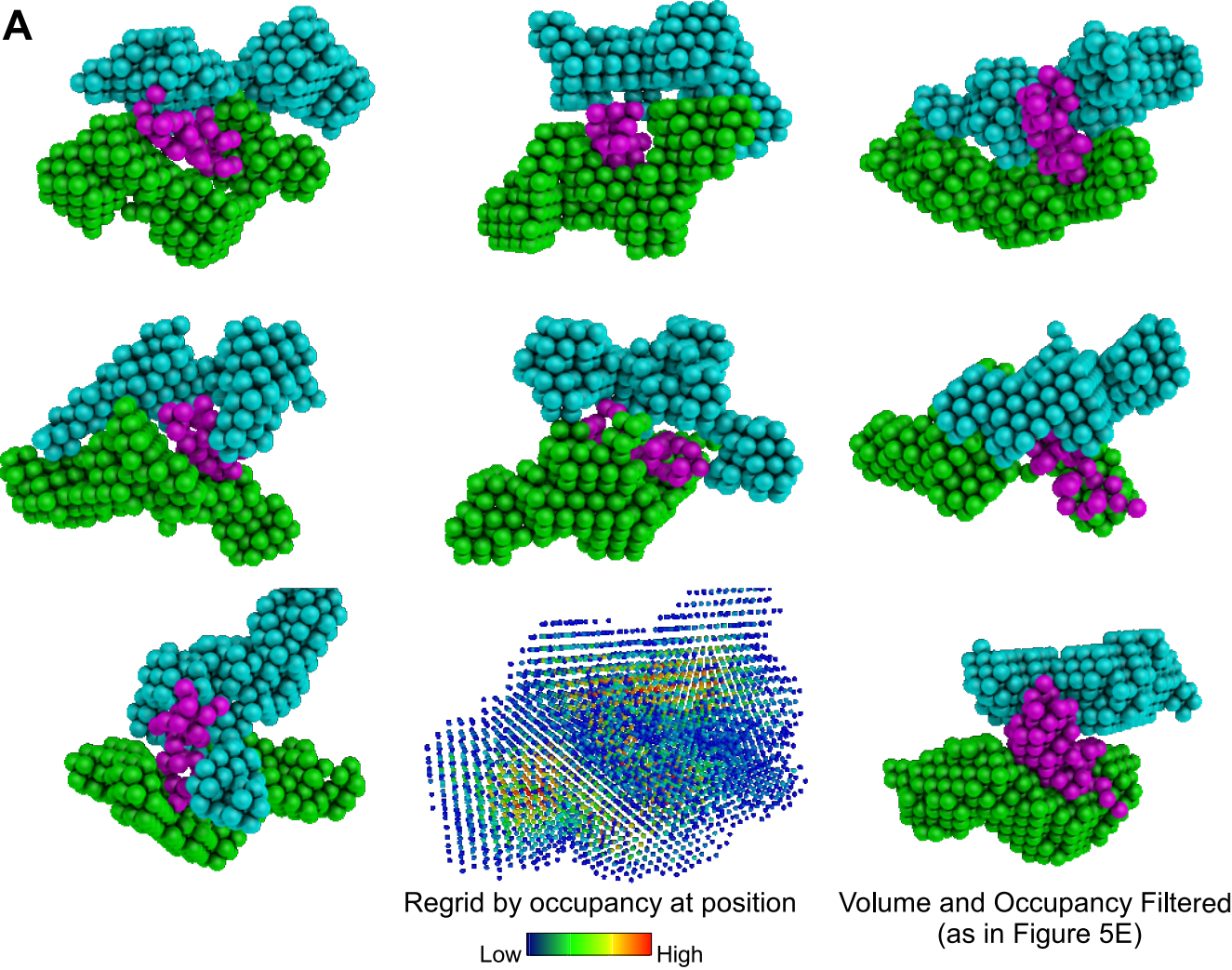
A
Regrid by occupancy at position
Low
High
Volume and Occupancy Filtered
(as in Figure 5E)

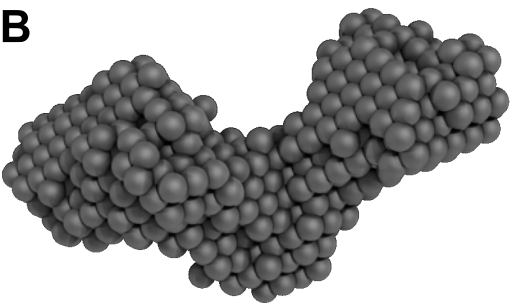
B

A

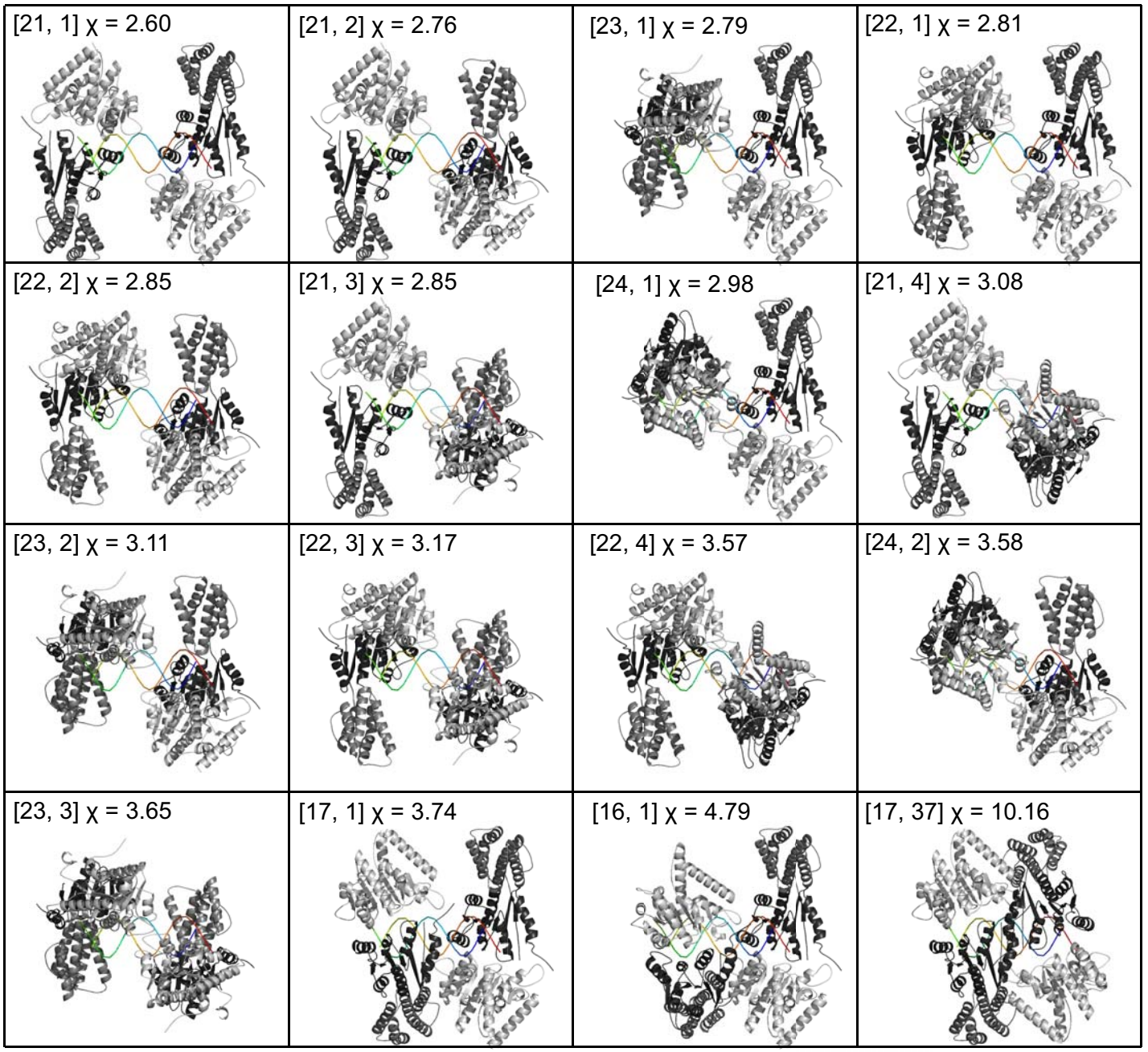

B

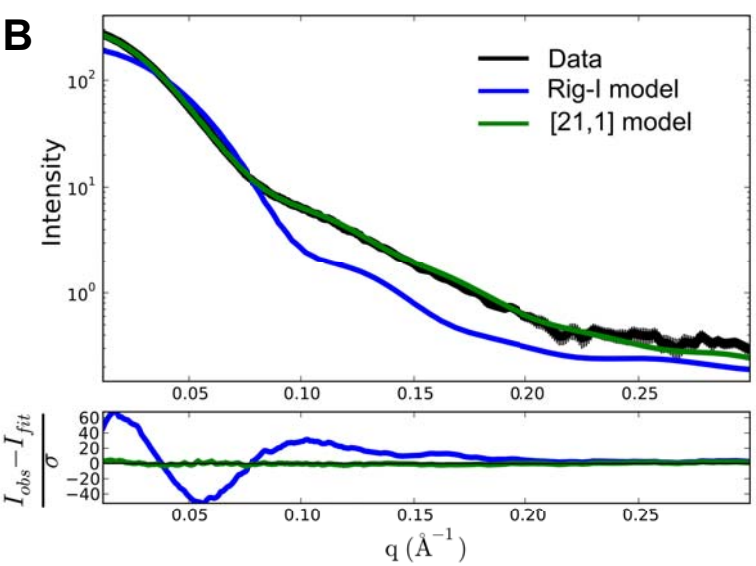

C

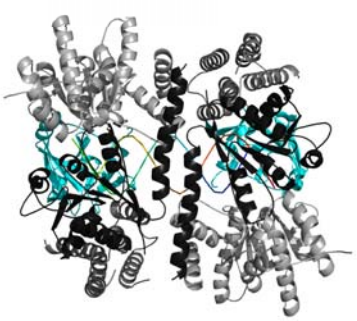

D

	R_g	D_{max}	χ
Rig-I based model	36.7	117	22.3
[21,1] refined model	47.3	163	1.35
SAXS Data	47.1	165	-

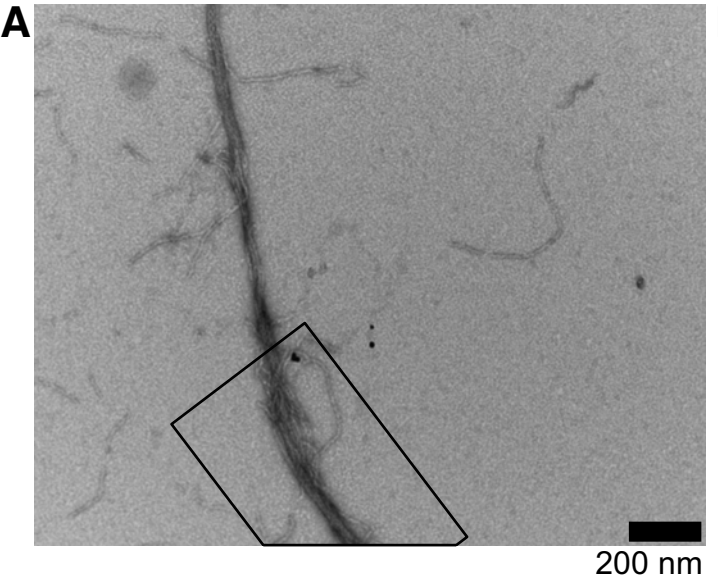
A
200 nm

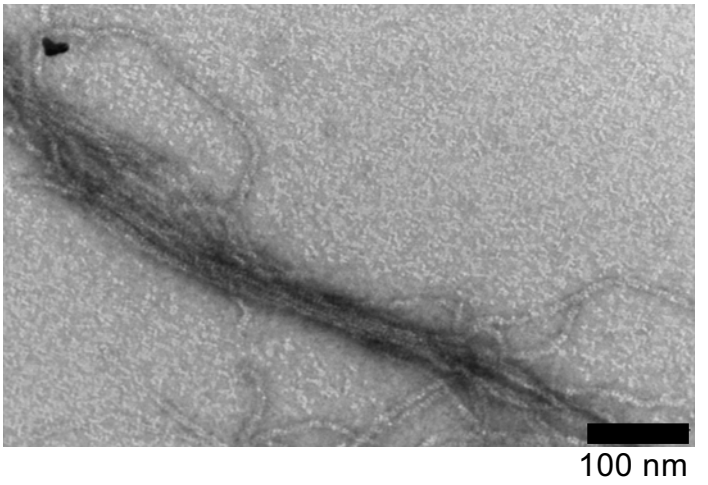
B
100 nm

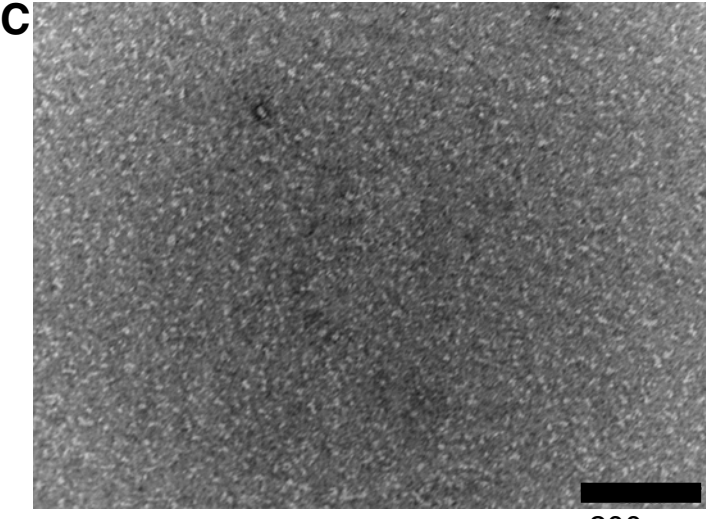
C
200 nm

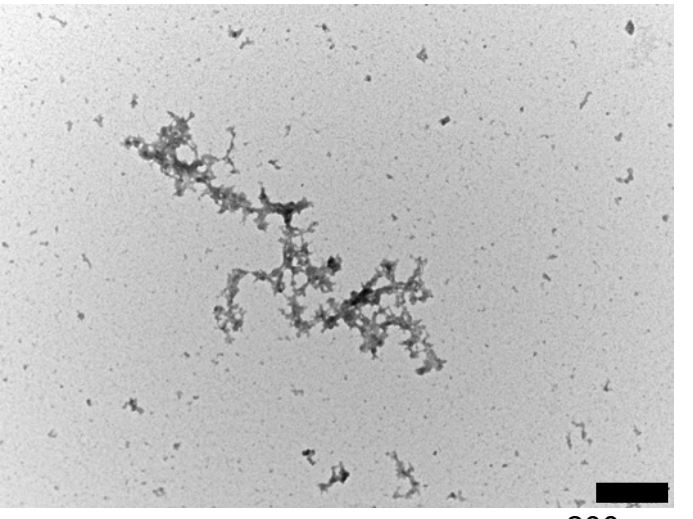
D
200 nm